LINEAR LOCAL BUCKLING OF THIN UHPC WALLS WITHOUT INTERMEDIATE STIFFENERS

*Jan Vesecký, *

Katedra betonových a zděných konstrukcí, Fakulta stavební,
České vysoké učení technické v Praze, Thákurova 7/2077, 166 29 Praha 6, Česká republika.
`jan.vesecky@fsv.cvut.cz`

ABSTRAKT

Moderní cementové kompozity, jako např. UHPC, umožňují výstavbu stále subtilnější prvků s tenkostěnnými průřezy, blížícími se svými proporcemi průřezům typickým pro ocelové konstrukce. S těmito prvky je ovšem spojena problematika ztráty stability dílčích stěn, které nebyla dosud u betonových konstrukcí věnována téměř žádná pozornost. Článek se proto zabývá jedním ze základních způsobů ztráty stability prvků s tenkostěnným průřezem – lokálním boulením stěn. Numerickými výpočty jsou stanoveny hodnoty kritického napětí vnitřních i okrajových stěn proměnné délky, vystavených tlakovému, ohybovému nebo smykovému namáhání za předpokladu lineárně pružné odezvy materiálu a nulových imperfekcí. Pro nejnižší hodnoty kritického napětí jsou odvozena kritéria maximální přípustné štíhlosti stěn z UHPC a v závěru článku jsou pro stěnu referenčních rozměrů stanoveny minimální přípustné tloušťky, potřebné pro zajištění stabilního chování.

KLÍČOVÁ SLOVA

Stabilita • Lokální boulení • Tenkostěnný průřez • Štíhlost • UHPC

ABSTRACT

Modern cementitious composites, such as UHPC, enable the construction of increasingly more slender elements with thin-walled cross sections resembling the proportions typical for steel structures. However, such members are subjected to the problem of loss of stability of individual walls. This problem has historically received little attention in the field of concrete structures. Therefore, this paper deals with one of the basic types of stability loss of thin-walled elements – local buckling. The critical stress values of variable length internal and outstanding walls, subjected to compression, bending, or shear loads assuming a linear elastic material response and zero imperfections, are determined by numerical analysis. For the lowest values of critical stress, criteria for the maximum admissible slenderness of UHPC walls are obtained, and finally the paper concludes with the minimum admissible thicknesses required to ensure stable behavior for a wall with reference dimensions.

KEYWORDS

Stability • Local buckling • Thin-walled cross-section • Slenderness • UHPC

1. INTRODUCTION

Most of the typical reinforced concrete (or prestressed concrete) beam members are designed with a solid cross section, stiff enough to prevent any potential stability failure. The same is true for most of the typical concrete columns, except the very slender ones, which may fail due to buckling. However, in general, for the majority of today's concrete structures, the stability check of individual members is not performed at all.

The situation changes considerably with the development of modern cementitious composites, most notably ultra-high performance concrete (UHPC). Due to its high compressive strength, significant tensile strength, and ductility (when compared to regular concrete), UHPC is suited for the design of members with (open or closed) thin-walled cross section. The thickness of individual walls of such a member can be as low as 25-30 mm (see Coufal et al., 2022 and Figure 1), comparable to a typical steel thin-walled cross-section.

Figure 1: *Completed thin-walled.UHPC structures:*
a) footbridge near Vrapice village (KŠ Prefa),
b) experimental footbridge with Pi-section (FHWA).

* Školitel: doc. Ing. Lukáš Vráblík, Ph.D., FEng.

Then, an important question naturally arises, whether such a member is stiff enough to reach its full capacity (strength failure), or whether it will earlier buckle (stability failure). There are multiple types of stability failure of thin-walled members.

1.1. Instabilities of thin-walled members

Slender columns and beams with a solid cross-section may lose only global stability, because the cross-section is highly rigid in its own plane. Therefore, the whole member (or its part between the lateral supports) buckles which usually leads to the collapse of the member. The types of global stability failure are

- Flexural buckling in compression;
- Torsional buckling in compression;
- Torsional-flexural buckling in compression;
- Lateral torsional buckling in bending.
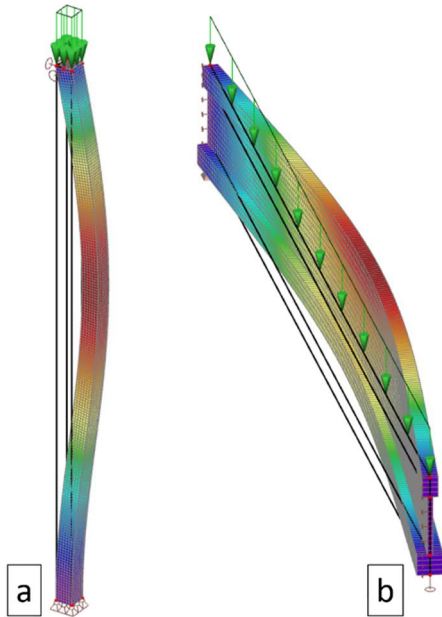
Examples are shown in Figure 2.

Figure 2: *Selected types of global instabilities*
a) flexural buckling, b) lateral torsional buckling.

While all mentioned global stability problems are relevant also for thin-walled members, additionally a loss of local stability may also occur. Then only a part of the cross-section buckles, while the rest may still be able to transfer loads. To identify local stability problems, cross-section of a member can no longer be assumed as rigid in its own plane, but instead must be considered as a set of interconnected walls. The types of local stability failure are:

- Local buckling;
- Distortional buckling;
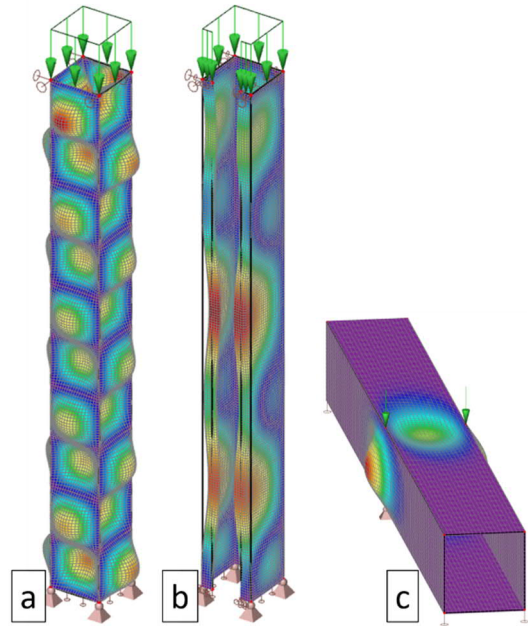- Web crippling.

Examples are shown in Figure 3.

Figure 3: *Types of local instabilities*
a) local buckling, b) distortional buckling, c) web crippling.

1.2. Transition from cross-section to individual walls

There is, in general, infinitely many shapes of thin-walled cross-sections. Therefore, it is impossible to analyze every shape and it is convenient to split thin-walled members into individual walls (see Figure 4) and analyze those instead. There exist only two major types of walls obtained from the decomposition of thin-walled members:

- Internal wall – supported along all edges;
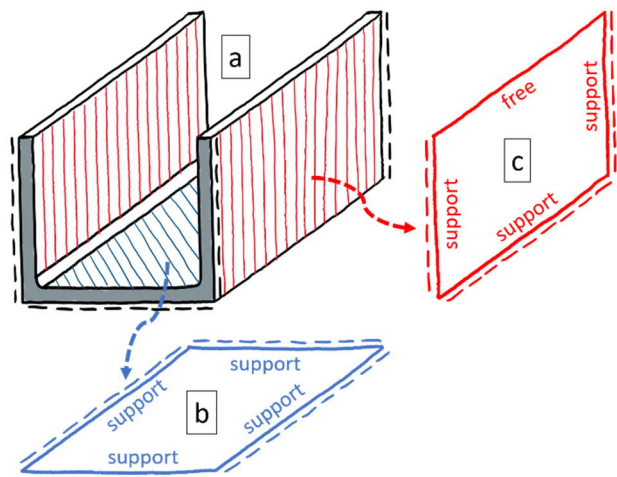- Outstand wall – supported along three edges and free along one logitudinal edge;

Figure 4: *Decomposition of the thin-walled member with stiffened ends: a) original member, b) internal wall, c) outstand wall.*

1.3. State of the art

The topic of local stability and especially the local buckling of thin walls is established for over a hundred years since the first formulation of the governing equations (see Section 2.1).

The problem is generally well researched and understood in the case of steel structures and the main conclusions and results may be found in multiple theoretical papers and monographs (for example, Timoshenko & Gere, 1961; Ziemian et al., 2010; Young et al., 2012) as well as design standards (for example EN 1991-1, Parts 1, 3 and 5). These results are derived from a wide range of linear and nonlinear numerical simulations as well as full-scale and reduced-scale experiments.

In contrast, there is currently very little knowledge about the local stability problems regarding the thin-walled cementitious composite members. This is most likely due to the fact that for many years it was virtually impossible to build actually thin-walled members. This situation changed in the last 20 years, with the first UHPC structures in the 2000s and especially with "bolder" UHPC (and TRC) structures in 2010s.

Only a few theoretical papers regarding the local buckling of UHPC thin-walled members have been published so far (Lee et al., 2021a; Lee et al., 2021b) and there are no provisions regarding local stability in any design codes and standards for concrete structures.

Thus, it is apparent that research in this topic is of high importance.

2. LOCAL BUCKLING

This paper is focused on the issue of local buckling, which is probably the most important type of local stability problem as listed in Section 1.1.

2.1. Theory – governing equations

To analyze the (local) buckling of a wall, it is necessary to link together in-plane wall theory (first introduced by George Biddell Airy in 1862 (published 1866)) and out-of-plane plate bending theory (first introduced by Marie Sophie Germain in 1816 (published 1821)). Assuming isotropic material properties, a set of fourth-order elliptic nonlinear partial differential equations (called Von Karman equations), is obtained (Föppl, 1907; Von Karman, 1910):

$$D_{ep} \cdot \left(\frac{\partial^4 w}{\partial x^4} + 2 \cdot \frac{\partial^4 w}{\partial x^2 \partial y^2} + \frac{\partial^4 w}{\partial y^4} \right) - E_t \cdot t_w \cdot$$
$$\cdot \left(\frac{\partial^2 \Phi}{\partial y^2} \cdot \frac{\partial^2 w}{\partial x^2} - 2 \cdot \frac{\partial^2 \Phi}{\partial x \partial y} \cdot \frac{\partial^2 w}{\partial x \partial y} + \frac{\partial^2 \Phi}{\partial x^2} \cdot \frac{\partial^2 w}{\partial y^2} \right) = f_z \quad (1)$$

$$\frac{\partial^4 \Phi}{\partial x^4} + 2 \cdot \frac{\partial^4 \Phi}{\partial x^2 \partial y^2} + \frac{\partial^4 \Phi}{\partial y^4} + \frac{\partial^2 w}{\partial x^2} \cdot \frac{\partial^2 w}{\partial y^2} - \left(\frac{\partial^2 w}{\partial x \partial y} \right)^2 = 0 \quad (2)$$

(+ *appropriate boundary conditions*)
where D_{ep} is the elastoplastic stiffness matrix, E_t is the tangential modulus of the material, t_w is the thickness of the wall, f_z is the lateral surface load, w is the load-induced deflection, calculated as the difference between the total deflection (w_{tot}) and the initial deflection due to imperfections (w_0), and finally Φ is the Airy stress function, from which the unit in-plane normal (n_x, n_y) and shear (n_{xy}) forces can be calculated as the second partial derivations, multiplied by the thickness t_w.

Von Karman equations can be in general geometrically and materially nonlinear, including the effect of damage by introducing the matrix Ω, containing the damage parameters ω in tension (cracks) and compression (crushing).

However, in this paper, only the linearized form of equations is investigated.

2.2. Linear local buckling

A linear form of Von Karman equations can be considered when the following requirements are fulfilled (in addition to the required isotropic properties):

- Zero lateral load ($f_z \equiv 0$)
- Linear elastic material response (i.e., constant modulus of elasticity and Poisson's ratio);
- No creep and/or shrinkage effects;
- "Perfect" wall without imperfections ($w_0 = 0$);
- Infinitezimal strains and displacements.

Then the Eqs. (1) and (2) can be combined into a single fourth-order linear homogeneous partial differential equation (Timoshenko & Woinowsky-Krieger, 1959):

$$D_{el} \cdot \left(\frac{\partial^4 w}{\partial x^4} + 2 \cdot \frac{\partial^4 w}{\partial x^2 \partial y^2} + \frac{\partial^4 w}{\partial y^4} \right) +$$
$$+ \left(n_x \cdot \frac{\partial^2 w}{\partial x^2} - 2 \cdot n_{xy} \cdot \frac{\partial^2 w}{\partial x \partial y} + n_y \cdot \frac{\partial^2 w}{\partial y^2} \right) = 0 \quad (3)$$

(+ *appropriate boundary conditions*)
where D_{el} is the elastic stiffness matrix.

The Eq. (3) represents a classical eigenvalue problem. Therefore, for the given homogeneous boundary conditions a pairs of eigenvalues and eigenfunctions can be found. Those represent the critical unit forces (n_{cr}) and the corresponding buckling shapes (w). Eigenvalues are usually represented in the form of critical stresses rather than critical unit forces, using a simple relation:

$$\sigma_{cr} = \frac{n_{cr}}{t_w} \quad (4)$$

In the most cases, the first (lowest) critical stress is the most important one.

It should be noted that the exact solution of an eigenvalue problem (Eq. (3)) can be found only for a very limited number of (special) cases, despite all simplifying assumptions. Therefore, only an approximate solution can be found in most cases, usually by using numerical methods (see Section 3.1).

2.3. Fundamental solution – simply supported wall

At first, it is important to investigate a case, for which an analytical solution can be found – an infinitely long wall ($l_w = \infty$) with a finite height (h_w) hinged on both longitudinal sides and loaded on the single longitudinal side by an uniform compressive force (n), see Figure 5.
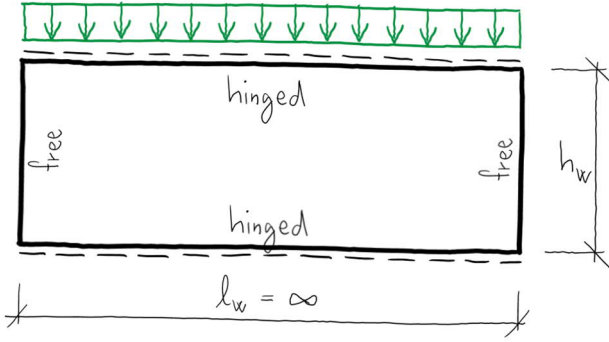
Figure 5: *Scheme of the simply supported wall subjected to uniform vertical compression.*

The analytical solution in such a case is similar to the analytical solution of a column with rectangular cross-section. Bending stiffnes of a rectangular cross-section with a width (b) and height conveniently denoted (t) can be calculated as:

$$D_{rectangle} = E \cdot I = \frac{E \cdot b \cdot t^3}{12} \tag{5}$$

where I is an axial moment of inertia of the cross-section.

Assuming that a rectangular cross-section is instead a unit strip of a plate (b = "1") with the thickness (t_w), the bending stiffness is slightly modified due to the effect of planar stress:

$$D_{plate} = \frac{E \cdot t_w^3}{12 \cdot (1 - \mu^2)} \tag{6}$$

where μ is Poisson's ratio of the material. For the typical structural materials, bending stiffness of a plate is higher, compared to the stiffnes of a rectangular cross section with the same width:

- Concrete (μ = 0,2) – 4,2 % stiffness increase;
- Steel (μ = 0,3) – 9,9 % stiffness increase;
- Perfectly plastic incompressible material (μ = 0,5) – 33,3 % stiffness increase.

Then, the first critical unit force (usually called Euler force) of a wall, corresponding to the first buckling mode (see Figure 6) is defined as:

$$n_E = \frac{\pi^2 \cdot D_{plate}}{h_w^2} = \frac{\pi^2 \cdot E \cdot t_w^3}{12 \cdot (1 - \mu^2) \cdot h_w^2} \tag{7}$$
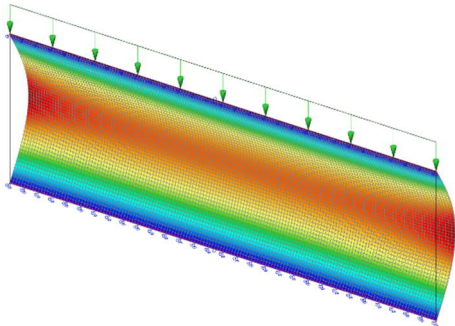

Figure 6: *First buckling mode of the simply supported wall subjected to the uniform vertical compression (result for the finite length of the wall).*

By dividing the uniform force by the thickness of a wall (t_w), a so-called Euler stress is obtained:

$$\sigma_E = \frac{n_E}{t_w} = \frac{\pi^2 \cdot E}{12 \cdot (1 - \mu^2)} \cdot \left(\frac{t_w}{h_w}\right)^2 \tag{8}$$

Let us define the slenderness of a wall as:

$$\lambda_w = \frac{h_w}{t_w} \tag{9}$$

And the Euler stress (Eq. (8)) can be finally expressed in the form:

$$\sigma_E = \frac{\pi^2 \cdot E}{12 \cdot (1 - \mu^2) \cdot \lambda_w^2} \tag{10}$$

which will be later useful for the derivation of the limiting slenderness of a wall with arbitrary boundary conditions.

2.4. Arbitrary configuration of boundary conditions

As stated before, a local buckling eigenvalue problem (Eq. (3)) cannot be solved analytically in the most cases. Thus, it is convenient to relate the solution of an arbitrary configuration of boundary conditions and an arbitrary type of loading to the value of Euler stress of the simply supported wall (Eq. (10)), provided that the wall is rectangular (with length l_w and height h_w) and without any openings. Such relation can be formulated as:

$$k = \frac{\sigma_{cr}}{\sigma_E} \tag{11}$$

where k is so-called linear local buckling factor. To distinguish normal and shear stress buckling, the linear local buckling factor is usually denoted either k_σ or k_τ, and the critical (normal/shear) stress can be expressed as:

$$\sigma_{cr} = k_\sigma \cdot \sigma_E \tag{12}$$

$$\tau_{cr} = k_\tau \cdot \sigma_E \tag{13}$$

Nevertheless, for the simplicity, throughout the rest of this paper, buckling factor will be denoted only as k.

3. LINEAR LOCAL BUCKLING FACTOR

As shown in the previous chapter, the linear local buckling factor (k) is one of the most important quantities describing the local buckling of the wall. Therefore, its values for the most practical cases of the UHPC walls are computed using the finite element method.

It is important to note that the linear local buckling factor is not a constant but rather that it is a function dependent on the length to height ratio of the wall (l_w/h_w). It is therefore expressed in the form of charts and then the minimum value (k_{min}) is evaluated for each type of boundary conditions and loading.

3.1. Numerical modelling

To find an approximate solution of an eigenvalue problem (Eq. (3)) a finite elements analysis was employed, using a general purpose software Scia Engineer 21.1. A problem with infinitely many degrees of freedom was therefore transformed

into a typical generalized eigenvalue problem of a matrix with a finite size, formally written as:

$$(K - \sigma_{cr} \cdot K_\sigma) \cdot w = 0 \qquad (14)$$

where K is the global stiffness matrix of the wall and K_σ is the global initial stress matrix.

A very fine square mesh was used for the analysis to ensure the minimum error of an approximate solution. Always at least 100 square elements was used in the direction of the shorter side of the wall, thus:

$$a_e \leq \frac{\min(h_w, l_w)}{100} \qquad (15)$$

where a_e is the size of the side of the square element.

A standard Cholesky decomposition was used to compute initial solution and global initial stress matrix. Subsequently, two different methods were used to solve the generalized eigenvalue problem (Eq. (14)):

- Lanczos method when multiple eigenvalues were desired, while the number of DOF was less than 1 million;
- Polynomial method when only a single (lowest) eigenvalue was desired and the number of DOF was greater than 0,5 million.

It was proven that those two methods were the fastest, while providing very accurate results (compared to each other as well as to other methods, e.g., subspace iteration or iterative ICGC).

3.2. Assumed boundary conditions

It was shown in Section 1.2 that an arbitrary thin-walled cross-section can be decomposed into a set of individual walls – either internal or outstand (see Figure 7).
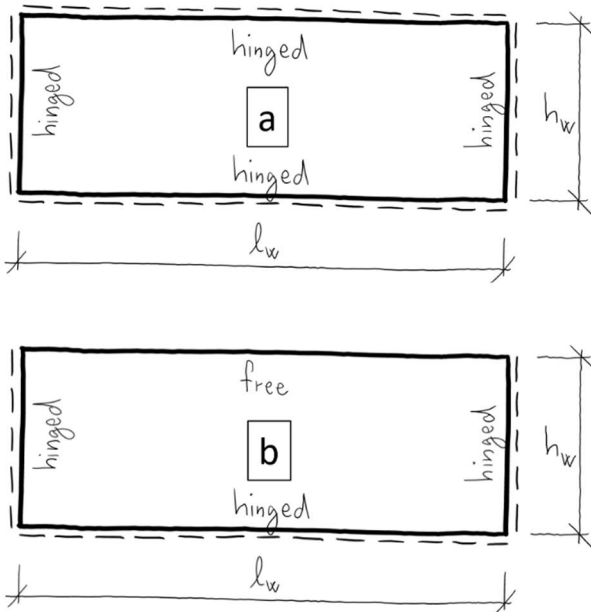

Figure 7: *Scheme of a) internal and b) outstand wall with hinged boundary conditions.*

The corners of the original cross-section where the walls are connected shall be replaced by boundary conditions along the longitudinal edge.

The most accurate representation of such a connection should be a combination of two springs – one providing partial out-of-plane rigidity, while the other providing partial rotational rigidity. However, the actual stiffness of those springs may vary from near-zero to almost infinity. In most cases, the provided out-of-plane rigidity is much higher than the rotational rigidity, thus it is reasonable to consider a perfectly rigid out-of-plane boundary condition without any rotational rigidity. Such boundary conditions will be furthermore called as *hinged*. It should be noted that if the connections do not provide enough out-of-plane rigidity, then the stability failure is called distortional buckling instead of local buckling and such a case is not considered in this paper.

Furthermore, in the case of an outstand wall, one of the longitudinal edges of the wall is not connected to any other wall, and then there should be no boundary conditions at all and such edge shall be called as *free*.

In relation to the trailing edges of the wall, simple stiffeners were considered on both sides, providing full out-of-plane restraint and zero rotational restraint. Therefore, *hinged* boundary conditions were imposed on both trailing edges.

No intermediate stiffeners were considered in this study.

3.3. Assumed types of loading

Generally, the loading of an individual wall can be arbitrarily complex, resulting in a complicated stress pattern, which may even vary along the longitude of the wall. However, as long as the linear behavior is maintained, any loading pattern can be constructed as a summation of basic loading types.

Therefore, in this paper only basic types of loading are considered, which produce an uniform stress pattern along the longitude of the wall (see also Figure 8). These are:

- Uniform compression;
- Uniform bending;
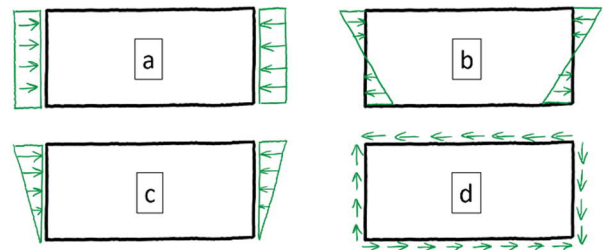- Compression-bending interaction;
- Uniform shear.

Figure 8: *Assumed types of loading;*
(a) uniform compression, b) uniform bending,
c) compression-bending interaction, d) uniform shear.

3.4. Assumed material properties

In Section 2.2, multiple requirements (assumptions) were listed to simplify the general governing equations of local buckling into a single governing equation of the linear local buckling.

It must be emphasized that those requirements are in general not fulfilled for the real thin-walled UHPC members:

- Modulus of elasticity and Poisson's ratio remain constant only prior to the first tensile crack and roughly prior to 70-80% of the compressive strength (Hamdy et al., 2014; Coufal et al., 2022);
- Material parameters may be even heterogeneous if the fiber reinforcement is predominantly oriented in one direction, for example, due to 3D printing (Yang et al., 2022);
- In the long term, the effect of creep and shrinkage is apparent;
- Wall is always imperfect and the magnitude of deflection may be comparable to the thickness of the wall (i.e., large displacements).

Hovewer, those sources of nonlinearity are not considered in this paper and therefore the results obtained in the next sections should be treated as the initial and partially overestimated approximation of the real local buckling strength of thin UHPC walls.

In this context, the following constant linear elastic material properties were considered:

- Modulus of elasticity $E = 50\ 000$ MPa;
- Poisson's ratio $\mu = 0{,}2$.

It will be shown later, that the resulting linear local buckling factor k is independent of the modulus of elasticity, but depends on the Poisson's ratio in some cases.

3.5. Uniform compression

Internal walls, hinged along all edges and subjected to the uniform compression acting in the longitudinal direction buckle in multiple square-shaped half-waves (see Figure 9 and Figure 11), while the minimum linear local buckling factor k_{min} is reached each time the l_w/h_w ratio reaches an integer value.
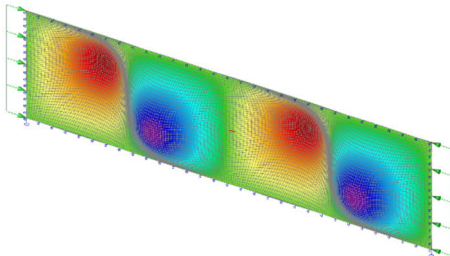

Figure 9: *Linear local buckling of the hinged internal UHPC wall, $l_w/h_w = 4$, subjected to uniform compression.*

Outstand walls hinged along three edges, free along a single longitudinal edge and loaded similarly buckle always in a single half-wave (see Figure 10 and Figure 11). However, for the infinitely long wall ($l_w/h_w = \infty$) the linear local buckling factor for any number of half-waves approaches the same value, which is also the minimum value k_{min}. Therefore, in practice, for a very long outstand wall, the stability failure may occur in any number of half-vawes.
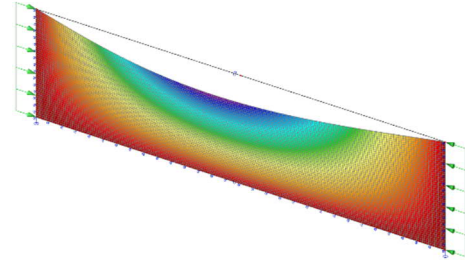

Figure 10: *Linear local buckling of the hinged outstand UHPC wall, $l_w/h_w = 4$, subjected to uniform compression.*
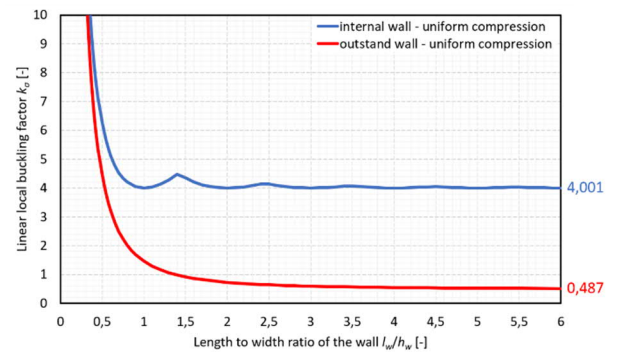

Figure 11: *Linear local buckling factor of the hinged internal/oustand UHPC wall subjected to uniform compression.*

3.6. Uniform bending

Internal wall, hinged along all edges and subjected to the uniform bending acting in the longitudinal direction buckles in multiple rectangle-shaped half-waves (see Figure 12 and Figure 16), while the minimum linear local buckling factor k_{min} is reached each time the l_w/h_w ratio reaches the multiple of 2/3.
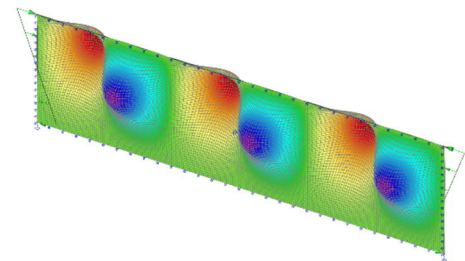

Figure 12: *Linear local buckling of the hinged internal UHPC wall, $l_w/h_w = 4$, subjected to uniform bending.*

In the case of an outstand wall, two significantly different types of uniform bending can be applied (see Figure 13):

- Negative bending – the compression is acting along the free edge;
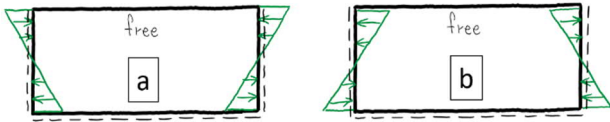- Positive bending – the compression is acting along the hinged edge.

Figure 13: *Outstand wall subjected to a) negative bending, b) positive bending.*

When negative bending is imposed, the observed behavior is similar to the one of uniform compression of the outstand wall. It tends to buckle always in a single half-wave (see Figure 14 and Figure 16), but for the infinitely long wall, any number of half-waves is possible as well as the minimum value k_{min} at that moment.
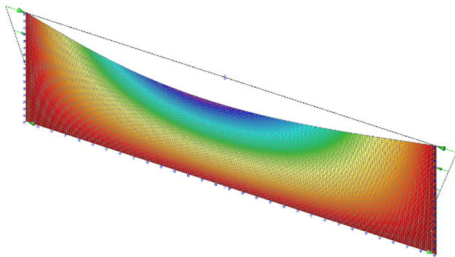

Figure 14: *Linear local buckling of the hinged outstand UHPC wall, $l_w/h_w = 4$, subjected to negative bending.*

In contrast, when positive bending is imposed, the free edge is „pretensioned" and the behavior is the same as in the case of internal wall and the buckling occurs in multiple rectangle-shaped half-waves (see Figure 15 and Figure 16).
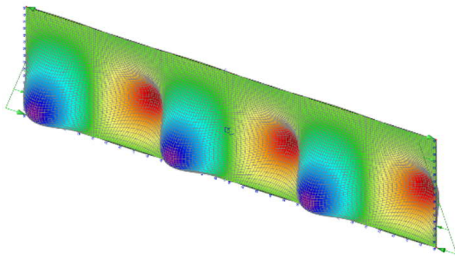

Figure 15: *Linear local buckling of the hinged outstand UHPC wall, $l_w/h_w = 4$, subjected to positive bending.*
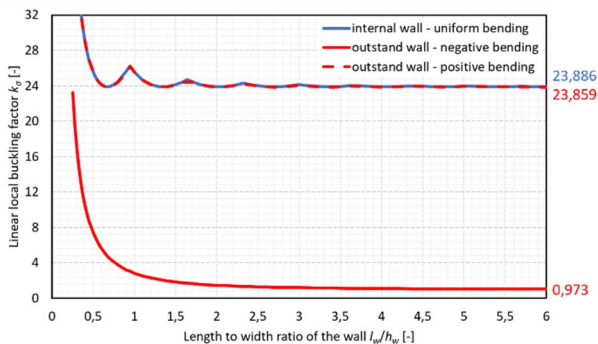

Figure 16: *Linear local buckling factor of the hinged internal/oustand UHPC wall subjected to uniform bending.*

3.7. Bending-compression interaction

In general, any ratio between bending- and compression-induced stress can be assumed. However, in this paper, only the case when 50% of the stress is caused by bending and 50% by compression is investigated. Such a combination results in a triangularly shaped stress pattern along the longitude of the wall, with maximum compressive stress along one longitudinal edge and zero stress along the other longitudinal edge.

The observed buckling patterns are similar to the uniform bending in the case of internal wall and outstand wall subjected to compression + negative bending (see Figure 17, Figure 18, and Figure 20).
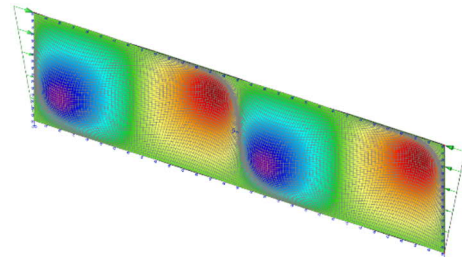

Figure 17: *Linear local buckling of the hinged internal UHPC wall, $l_w/h_w = 4$, subjected to 50% compression-bending interaction.*
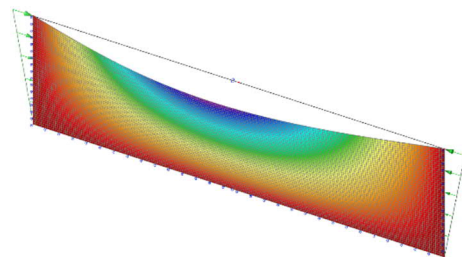

Figure 18: *Linear local buckling of the hinged outstand UHPC wall, $l_w/h_w = 4$, subjected to 50% compression-negative bending interaction.*

However, in the case of an outstand wall subjected to compression + positive bending, the free edge is no longer pretensioned and therefore the wall tends to always buckle in a single half-wave (see Figure 19 and Figure 20).
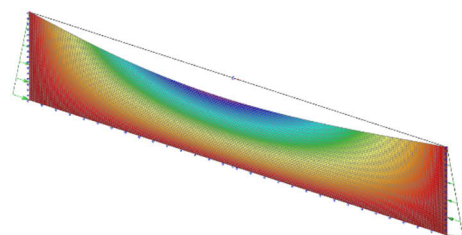

Figure 19: *Linear local buckling of the hinged outstand UHPC wall, $l_w/h_w = 4$, subjected to 50% compression-positive bending interaction.*
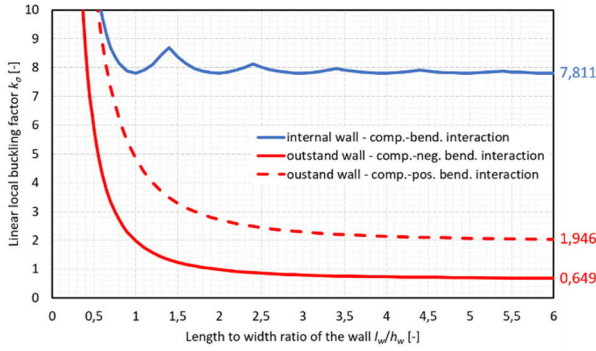
Figure 20: *Linear local buckling factor of the hinged internal/oustand UHPC wall subjected to 50% compression-bending interaction.*

3.8. Uniform shear

Internal walls hinged along all edges and subjected to a uniform shear buckle with multiple diagonally oriented half-waves (see Figure 21 and Figure 23). However, the minimum linear local buckling factor k_{min} is not reached multiple times, as in the case of compression and bending, but only once for the infinitely long wall.
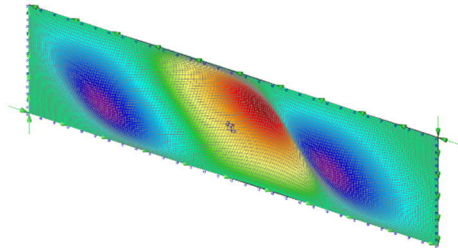

Figure 21: *Linear local buckling of the hinged internal UHPC wall, $l_w/h_w = 4$, subjected to uniform shear.*

In the case of outstand walls, a single half-wave buckling always occurs as the first (see Figure 22 and Figure 23) except for very short walls with the ratio $l_w/h_w \leq 0,7$ when multiple half-waves may occur.
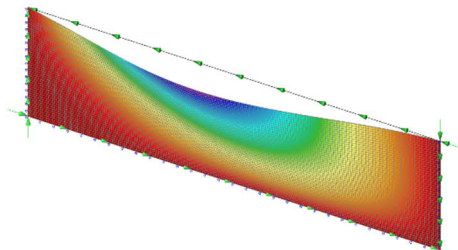

Figure 22: *Linear local buckling of the hinged outstand UHPC wall, $l_w/h_w = 4$, subjected to uniform shear.*
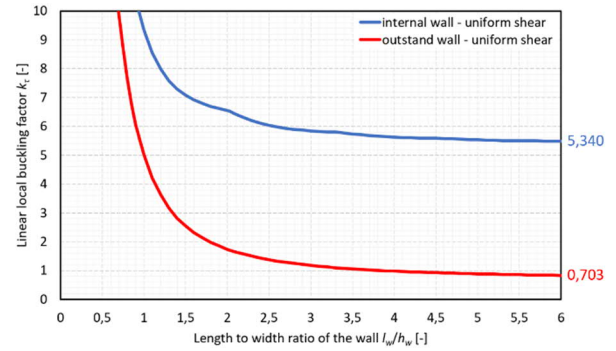

Figure 23: *Linear local buckling factor of the hinged internal/oustand UHPC wall subjected to uniform shear.*

3.9. Minimum linear local buckling factor

In most of the cases, members with thin-walled cross-section are usually relatively long, thus the length of an individual wall is significantly greater than its height, i.e., $l_w/h_w \gg 1$. Therefore, it is often reasonable to consider the minimum possible value of the linear local buckling actor k_{min}, rather than using the exact value, which is just slightly higher.

For that reason, the values of the minimum linear local buckling factor k_{min} are summarized in Table 1. In theory, those values are generally reached for the limit case $l_w/h_w = \infty$, however, due to the numerical solution those values were computed for the ratio $l_w/h_w = 75$. The difference is negligible.

Table 1: *Minimum linear local buckling factor of the internal/oustand UHPC walls with hinged edges and subjected to different types of loading.*

Loading	k_{min} [-]	
	Internal	Outstand
Compression	4,001	0,487
Comp. + negative bending	7,811	0,649
Negative bending	23,886	0,973
Comp. + positive bending	-	1,946
Positive bending	-	23,859
Shear	5,340	0,703

3.10. Comparison of UHPC and steel walls

It was stated in Section 1.3 that while there is currently almost no literature regarding local buckling of thin-walled UHPC members (or members made out of cementitous composites in general), there is, in contrast, a wide range of sources regarding local buckling of thin-walled steel members. Therefore, it is convenient to compare UHPC results presented in this paper with steel results from the literature (Timoshenko & Gere, 1961; Ziemian et al., 2010; Young et al., 2012; EN 1993-1-5, 2006), see Table 2.

It is apparent from the table that the linear local buckling factor is identical for UHPC and steel in the case of internal walls, therefore it is indepdennt of both the modulus of elasticity and Poisson's ratio of the material.

Table 2: *Comparison of minimum linear local buckling factor for UHPC and steel internal and outstand walls.*

| | k_{min} [-] | | | |
| | Internal | | Outstand | |
Loading	UHPC	Steel	UHPC	Steel
Compression	4,001	4,00	0,487	0,43
Comp. + neg. bend.	7,811	7,81	0,649	0,57
Negative bending	23,886	23,9	0,973	0,85
Comp. + pos. bend.	-	-	1,946	1,70
Positive bending	-	-	23,859	23,8
Shear	5,340	5,34	0,703	0,66

In contrast, the linear local buckling factor differs for UHPC and steel in the case of oustand walls, with UHPC being higher. The only exception is the outstand wall subjected to positive bending, which behaves similarly to the internal wall subjected to uniform bending. It can be shown that the difference in the values of linear local buckling factor is caused only by the different Poisson's ratio of both materials, while the modulus of elasticity does not influence the results.

Therefore, it can be concluded that the results related to the linear local buckling of internal steel walls can be directly adopted and applied for internal UHPC walls. Contrary, the linear local buckling of outstand UHPC walls must be addressed individually due to the different Poisson's ratio compared to steel.

In addition, it is shown that the linear local buckling factor of the outstand walls is inversely proportional to the Poisson's ratio of the material.

4. LIMITING SLENDERNESS OF THE WALL

It is of high practical importance to utilize linear local buckling factors from the previous chapter to distinguish between thin UHPC walls that may and may not lose stability due to local buckling prior to reaching compressive strength (or tensile stregth in the case of bending and shear). The universal quantity for such distinction is limiting slenderness of the wall $\lambda_{w,lim}$.

It can be calculated first by the assumption of equilibrium between the strength of the material and the critical buckling stress, i.e., the case when both types of failure occur at once.

$$f = \sigma_{cr} = k \cdot \frac{\pi^2 \cdot E}{12 \cdot (1 - \mu^2) \cdot \lambda_w^2} \tag{16}$$

From this equation, by rearrangement of variables, the limiting slenderness of the wall can be evaluated:

$$\lambda_{w,lim} = \sqrt{k} \cdot \sqrt{\frac{\pi^2}{12 \cdot (1 - \mu^2)}} \cdot \sqrt{\frac{E}{f}} \tag{17}$$

When the actual slenderness of the wall is higher than the limiting slenderness, it will fail due to linear local buckling prior to the strength failure.

Because the Eq. (17) depends on the modulus of elasticity and the strength of the material, it is not possible to tabulate the resulting limiting slenderness for each type of boundary conditions and loading. This problem is addressed in the next two sections.

4.1. Limiting slenderness of the wall with referential material parameters

While the value of Poisson's ratio of all UHPC mixtures can be in general assumed as $\mu = 0,2$ (Hamdy et al., 2014), the strength f and the modulus of elasticity E may vary significantly. Therefore, it is beneficial to express the limiting slenderness of the wall with referential material parameters and then later modify its value by suitably selected coefficients.

Referential material parameters can be chosen arbitrarily. In this paper, they were chosen as follows:

$$E_{ref} = 50\,000\,MPa \tag{18}$$

$$f_{c,ref} = 150\,MPa \tag{19}$$

$$f_{t,ref} = 10\,MPa \tag{20}$$

where E_{ref} is the referential modulus of elasticity, $f_{c,ref}$ is the referential compressive strength, and $f_{t,ref}$ is the referential tensile strength.

By substituting Eqs. (18) and (19) into the Eq. (17) the limiting slenderness of the "referential" UHPC wall subjected to compression can be evaluated as:

$$\lambda_{w,c,ref,lim} = 16,8991 \cdot \sqrt{k} \tag{21}$$

and by substituting and Eqs. (18) and (20) into the Eq. (17) the limiting slenderness of the "referential" UHPC wall subjected to tension or shear can be evaluated as:

$$\lambda_{w,t,ref,lim} = 65,4498 \cdot \sqrt{k} \tag{22}$$

4.2. Generalized limiting slenderness of the wall

With known limiting slenderness of the referential wall, it is convenient to finally express the limiting slenderness of the wall with arbitrary material parameters by employing referential material parameters and expanding Eq. (17) in the following form:

$$\lambda_{w,lim} = \sqrt{k} \cdot \sqrt{\frac{\pi^2}{12 \cdot (1 - \mu^2)}} \cdot \sqrt{\frac{E_{ref}}{f_{ref}}} \cdot \sqrt{\frac{E}{E_{ref}}} \cdot \sqrt{\frac{f_{ref}}{f}} \tag{23}$$

The last two ratios from the equation can be denoted as the coefficient of real modulus of elasticity (c_E) and the coefficient of real strength (c_f):

$$c_E = \sqrt{\frac{E}{E_{ref}}} \tag{24}$$

$$c_f = \sqrt{\frac{f_{ref}}{f}} \tag{25}$$

Then the Eq (23) can be written as:

$$\lambda_{w,lim} = \sqrt{k} \cdot \sqrt{\frac{\pi^2}{12 \cdot (1 - \mu^2)}} \cdot \sqrt{\frac{E_{ref}}{f_{ref}}} \cdot c_E \cdot c_f \tag{26}$$

and finally evaluated using Eqs. (21) and (22) and the appropriate type of the reference strength (compressive or tensile):

$$\lambda_{w,c,lim} = 16,8991 \cdot \sqrt{k} \cdot c_E \cdot c_f \tag{27}$$

$$\lambda_{w,t,lim} = 65,4498 \cdot \sqrt{k} \cdot c_E \cdot c_f \tag{28}$$

In the case of both tensile and compressive stress acting on the wall at once (i.e. bending), both equations need to be evaluated and the value of the limiting slenderness which corresponds to the type of strength failure, that would occur as the first, should be used.

By evaluating Eqs. (27) and (28), assuming all loading cases described in the Sections 3.5 to 3.8 and selecting minimum possible values of the linear local buckling factor k_{min} from the Table 1 a conservative values of limiting slenderness of the wall can be derived, which are summarized in the Table 3.

Table 3: *Limiting slenderness of the internal/outstand UHPC walls with hinged edges and subjected to different types of loading.*

| Loading | Failure | $\lambda_{w,lim}$ [-] | |
		Internal	Outstand
Compression	C	**33,80**$\cdot c_E \cdot c_f$	**11,79**$\cdot c_E \cdot c_f$
Comp. + neg. b.	C	**47,23**$\cdot c_E \cdot c_f$	**13,61**$\cdot c_E \cdot c_f$
Negative bending	C	**82,59**$\cdot c_E \cdot c_f$	**16,67**$\cdot c_E \cdot c_f$
	T	**319,87**$\cdot c_E \cdot c_f$	**64,56**$\cdot c_E \cdot c_f$
Comp. + pos. b.	C	-	**23,57**$\cdot c_E \cdot c_f$
Positive bending	C	-	**82,54**$\cdot c_E \cdot c_f$
	T	-	**319,69**$\cdot c_E \cdot c_f$
Shear	T	**151,24**$\cdot c_E \cdot c_f$	**54,88**$\cdot c_E \cdot c_f$

5. LIMITING THICKNESS OF THE WALL

In the previous chapter, the limiting slenderness of the walls subjected to different types of loading was evaluated. It is then also possible to easily evalue the limiting thickness $t_{w,lim}$ by combining Eqs. (9) and (26) and rearranging the variables:

$$t_{w,lim} = \frac{h_w}{\lambda_{w,lim}} = \frac{h_w}{\sqrt{k} \cdot \sqrt{\frac{\pi^2}{12 \cdot (1 - \mu^2)}} \cdot \sqrt{\frac{E_{ref}}{f_{ref}}} \cdot c_E \cdot c_f} \qquad (29)$$

5.1. Wall with referential material parameters and dimensions

In the Table 4, the limiting thickness from the Eq. (29) is evaluated assuming referential material parameters as defined by Eqs. (18) to (20) and by assuming referential height:

$$h_{w,ref} = 1000\ mm \qquad (30)$$

Table 4: *Limiting thickness of the referential internal/outstand UHPC walls with hinged edges and subjected to different types of loading.*

| Loading | Failure | $t_{w,ref,lim}$ [mm] | |
		Internal	Outstand
Compression	C	**29,6**	**84,8**
Comp. + neg. b.	C	**21,2**	**73,5**
Negative bending	C	**12,1**	**60,0**
	T	**3,1**	**15,5**
Comp. + pos. b.	C	-	**42,4**
Positive bending	C	-	**12,1**
	T	-	**3,1**
Shear	T	**6,6**	**18,2**

It is apparent that the outstand wall subjected to compression, negative bending, or a combination of both is the most susceptible to local buckling, while the internal wall subjected to bending or shear is the least likely to buckle.

5.2. Arbitrary wall

Finally, it is possible to easily calculate limiting thickness of an arbitrary rectangular UHPC wall using values from the Table 4 and by defining the coefficient of the real height of the wall as:

$$c_h = \frac{h_w}{h_{w,ref}} \qquad (31)$$

Then the limiting thickness can be calculated as:

$$t_{w,lim} = t_{w,lim,ref} \cdot \frac{c_h}{c_E \cdot c_f} \qquad (32)$$

6. IMPORTANT REMARKS

It is important to recall that all results presented in this paper and especially the limiting slenderness and thickness of the wall provided in Table 3 and Table 4 were calculated with the assumptions in Section 2.2 related to the linear behavior. Behavior of the real thin-walled UHPC members is highly nonlinear (both materially and geometrically).

Thus, the obtained limiting slenderness and thickness represent the first approximation and the theoretical upper limit, which can never be reached for the real structures and therefore the presented results should be used with knowledge of this limitation.

Secondly, the coefficients c_E and c_f (Eqs. (24) and (25)) include the real modulus of elasticity and the real strength of UHPC. However, it is not mentioned which type of material parameters (in terms of statistics) should be used. While it is up to each engineer to use the most appropriate values, it is recommended to use 5% quantile of the modulus of elasticity and the 95% quantile of strength. Such a combination of material parameters provides the safest estimate of the limiting slenderness/thickness of the wall.

7. CONCLUSIONS

In this paper, a relatively new and underresearched topic of the local stability of thin-walled UHPC members was addressed, focusing especially on the issue of linear local buckling of individual walls under compression, bending and shear. The importance of this topic is most likely to grow significantly in the near future.

It was shown that the linear local buckling factor k is independent of the modulus of elasticity as well as Poisson's ratio of the material in the case of hinged internal wall, but that it is dependent on the Poisson's ratio in the case of hinged outstand wall. Therefore, it is not possible to adopt the results from the extensive literature on the topic of local buckling concerning steel structures.

For a total of 10 combinations of boundary conditions and types of loading, a limiting slenderness and limiting thickness of UHPC walls was calculated, assuming a minimum value of

the linear local buckling factor k_{min}. These results may be used as the useful first estimate (upper bound) for the local stability check of thin-walled UHPC members.

8. FUTURE REASEARCH

The author's future research regarding this topic is going to be focused on the extension and generalisation of the results presented in this paper, with respect to the linear local buckling.

Furthermore, the research is also going to account for the nonlinear behavior of thin-walled UHPC members and therefore ultimately to establish the real (nonlinear) values of the limiting slenderness subjected to an arbitrary type of loading.

ACKNOWLEDGEMENTS

References

Airy, G. B. (1866), *An Elementary Treatise on Partial Differential Equations*, London and Cambridge: MacMillan and Co.

Coufal, R., Kalný, M., Kolísko, J. & Vítek, J. L. (2022), *Technická pravidla ČBS 07 – Ultra vysokohodnotný beton (UHPC)*, Česká betonářská společnost ČSSI

EN 1993-1-1 (2005), Eurocode 3: *Design of steel structures – Part 1-1: General rules and rules for buildings*. Brussels: CEN

EN 1993-1-3 (2006), Eurocode 3: *Design of steel structures – Part 1-3: Supplementary rules for cold-formed members and sheeting*. Brussels: CEN

EN 1993-1-5 (2006), Eurocode 3: *Design of steel structures – Part 1-5: Plated structural elements*. Brussels: CEN

Föppl, A. (1907). *Vorlesungen Über Technische Mechanik*, Druck und Verlag von B.G. Teubner

Germain, M. S. (1821), *Recherches sur la théorie des surfaces élastiques*, , Paris: M.me v.e Courcier

Hamdy, K. S. E. et al. (2014), Mechanical properties of Ultra-High Performance Fiber Reinforced Concrete. *Int. Journal of Engineering and Innovative Technology* **4**(4), pp. 4-10

Lee, J. et al. (2021a), 'Theoretical Local Buckling Behavior of Thin-Walled UHPC Flanges Subjected to Pure Compression', *Materials* **14**(9), 2130

Lee, J. et al. (2021b), 'Experimental and numerical evaluations of local buckling in thin-walled UHPFRC flanges', *Thin-Walled Structures*, Vol. 163, 107662

SCIA Engineer, Documentation, available at: https://kc.scia.net/Documentation/

Timoshenko, S. P. & Gere, J. M. (1961), *Theory of Elastic Stability*, 2nd ed., New York: McGraw-Hill, ISBN: 978-0-486-47207-2

Timoshenko, S. P. & Woinowsky-Krieger, S. (1959), *Theory of Plates and Shells*, 2nd ed., McGraw-Hill, ISBN: 0-07-085820-9

Von Karman, T. (1910). *Festigkeitsprobleme im Maschinenbau*, In: 'Encyklopädie der Mathematischen Wissenschaften', Druck und Verlag von B.G. Teubner, pp. 311-385

Young, W. C., Budynas, R. G. & Sadegh, A. M. (2012), *Roark's Formulas for Stress and Strain*, 8th ed., McGraw-Hill, ISBN: 978-0-07-174248-1

Ziemian, R. D. et al. (2010), *Guide to Stability Design Criteria for Metal Structures*, 6th ed., New Jersey: John Wiley & Sons, ISBN: 978-0-470-08525-7